Indian Journal of Engineering & Materials Sciences
Vol. 29, February 2022, pp. 29-44

Characterization of finished surface through thermal additive centrifugal abrasive flow machining for better surface integrity

Parvesh Ali[a], R S Walia[b*], Qasim Murtaza[c], & Ranganath Muttanna Singari[d]

[a, c, d]Mechanical Department, Delhi Technological University, Delhi 110 042, India

[b]Department of Production and Industrial Engineering, Punjab Engineering College, Chandigarh 160 012, India

Received: 07 February 2019 ; Accepted: 8 October 2021

Abrasive Flow Machining (AFM) process has been a useful technique for deburring and polishing of the surface and edges through the abrasive laden media. The surface material has been removed in form of micro chips due to abrasion action of sharp cutting edges abrasive particles. A large amount of force and energy has been lost due to frictional forces between the surface and abrasive particles in AFM process. A new hybrid form of AFM process named as thermal additive centrifugal abrasive flow machining (TACAFM) has been discussed in the present investigation, which utilized the spark energy to melt the surface material. A lesser amount of force has been required by the abrasive particles to remove the molten material from the surface and also minimized the energy loss. In the present investigation central composite design response surface methodology has been used to plan and conduct the experiments using Design Expert® 11 software. Experiments have been performed to analyze the effect of input process variables such as current intensity, duty cycle, abrasive concentration, rotational speed of the electrode and extrusion pressure on scatter of surface roughness, micro hardness and % improvement in R_a of the workpiece. Also the finished surface of the brass work piece has been characterized for the microstructure study using SEM and XRD analysis. From the experimental results it has been found that duty cycle has the most significant effect towards Scatter of surface roughness with a contribution of 17.5 % while current has been contributed largest as 85.17 % towards micro hardness. Also it has been observed that current has contributed largest as 21.88% against the % improvement in R_a. The optimum scatter of surface roughness, micro hardness and % improvement in R_a has been observed as 0.15 µm, 345.95 HV and 39.52 % respectively.

Keywords: Abrasive Flow Machining (AFM), Abrasives, Finishing, Hardness, Scanning Electron Microscopy (SEM), X-Ray Diffraction (XRD), Machining, Spark

1 Introduction

In the present situation mechanical components having better functional performance and dimensional accuracy are highly demanded. It has developed competitiveness among various industries to produce better products with economic viability and good surface integrity. In recent past, industries used conventional techniques such as lapping, honing and broaching. However, these processes were very slow and had difficulty in machining the complex shapes. This leads to the evolution of nonconventional finishing processes, such as Abrasive Flow Machining (AFM). AFM is a micro/ nano finishing process used for deburring and polishing of the complex surfaces which cannot be achieved by conventional techniques [1, 2]. It used an abrasive laden media which is a combination of polymer, gel and abrasive particles, and passed through the restrictive passage with a high extrusion pressure. The abrasive laden media is viscous enough to hold the abrasive particles together during the finishing. The sharp cutting edge particles get in contact with the finishing surface and remove material in the form of micro/nano chips. AFM process has an advantage of less processing time and takes approximately only 10 percent of finishing time compared to the conventional technique [3]. In present scenario, AFM has numerous applications and is widely used to finish intricate shapes. Subramanian and Balashanmugam have reported the use of AFM technique for a wide variety of products including aircraft shuttle valves, propellers, dies etc. and stated that it is a flexible process and can be used for variety of materials[4]. Han *et al.*[5] used AFM process for the finishing of 15-5 PH stainless steel internal channels and observed the residual stress profile over the surface. It was found that AFM process produces compressive stress over the surface due to the generation of lesser temperature as compared to grinding and turning. Tzeng *et al.*[6] finished stainless steel (SUS 304) having

*Corresponding author (E-mail:waliaravinder@yahoo.com)

micro slit of width in the range of 0.23± 0.02 mm and concluded that the optimum machining quality was obtained at abrasive grain size of 150 μm, 50 percent of abrasive concentration, and 6.7 MPa of extrusion pressure. Sushil *et al.*[7] finished Al/SiC MMCs using AFM technique and optimized the parameters for material removal. The author concluded that workpiece material and extrusion pressure has a significant effect on material removal.

Furthermore, AFM process parameters such as pressure, abrasive concentration in media and viscosity of media were studied to optimize material removal and surface finish by many researchers [8-20]. Wan *et al.*[8] analyzed slip line velocity and wall shear stress for different values of extrusion pressure with two elliptical cross sections. It was stated that for low variation in cross section, zero order methodology was used and for larger variation order chronology was taken into consideration. Chen *et al.*[9] proposed a model on CFD-ACE software for different passageways of media flow and concluded that the helical passageways were better in comparison to polygonal passageways. Fu *et al.*[10] proposed a simulation on AFM process and concluded that an irregular stream line occurs at the leading as well as trailing edges in the media flow direction. Mali *et al.*[11] claimed through experimental results that abrasive mesh size has a significant effect on the material removal. Lv *et al.*[12] studied about the erosion mechanism of hard brittle materials during the finishing process and concluded that radial and lateral cracks were the main modes of fracture during the finishing. Wang *et al.*[13] sharpened the cutting edges of different coated and uncoated milling cutter using AFM process. The researchers observed that micro sized diamond film increases the roughness of rake and flank faces which correspond to reduction in radius of cutting edges. Shao and Cheng [14]studied about the surface roughness and topography profile during the AFM finishing process and observed that volume of abrasive media develops a huge difference in the machining system.

A number of development and modification was done in AFM process to enhance machining process productivity such as how to increase abrasive motion effectiveness, material removal, and surface integrity. Sankar *et al.*[15-16] developed Rotational AFM, which involved workpiece rotation through the gears to produce a centrifugal effect in the flowing media for the better contact of the abrasive particles with the finishing surface. The researcher also used a drill bit in the media path, which made the media to flow through the flutes of drill and increased number of active abrasive particles. This resulted in improvement of material removal from the surface. Brar *et al.*[17] developed Helical AFM process and optimized process parameters using Taguchi method. It was found from the experimental results that using stationary drill bit in the media flow path significantly improved material removal. Walia *et al.*[18] provided centrifugal motion to the abrasive laden media by rotating the flute rod in the centre of media and concluded that Centrifugal assisted AFM gave better surface in comparison to conventional AFM after specific number of cycles. Marzban *et al.*[19] used spin motion of the media along with the workpiece rotation during the finishing process in AFM and observed increase in material removal. Tzeng *et al.*[20]finished a micro channel by using self-modulating abrasive media. The author claimed that the highly concentrated coarse abrasive particles gave good level of finish.

It was concluded that AFM process cannot be used for larger surface irregularities because it removes material uniformly from the surface [21]. Although this process provided good surface finish but it had a constraint of low material removal. To remove these limitations the researchers are now trying to hybridize the process with other conventional and non-conventional techniques. Through various ongoing advanced finishing processes it seems that there is a scope of developing new techniques by hybridizing AFM process with other non-conventional processes to get better surface integrity. Therefore, the main objective of this paper was to develop such a hybrid process which can increase the material removal and produce better finished products. The developed technique is termed as Thermal additive Centrifugal Abrasive Flow Machining (TACAFM) process in which Centrifugal force assisted AFM (CFAAFM) is clubbed with EDM process to enhance the material removal and surface finish. The developed technique is operated at low pressure in comparison to the Conventional AFM process because the flow is restricted more in TACAFM process due to electrode rotation. Response surface Methodology was used to conduct the experiments on the developed Thermal additive Centrifugal AFM (TACAFM) setup for variable parameters to optimize process parameter for scatter of surface roughness, micro-hardness and percentage improvement in R_a.

2 Materials and Methods

2.1 Mechanism of Material Removal in TACAFM Process

AFM has a constraint of low material removal. It can be reduced by hybridizing AFM process with other nonconventional processes. In AFM process a huge amount of force was exerted by the abrasive particles for removing the material from the surface. Also a part of energy was lost due to friction between the sharp cutting edges and surface. This leads to the development of such a hybrid process which can reduce the energy loss and improves the material removal.

Thermal additive Centrifugal AFM (TACAFM) was a hybridization of conventional AFM with a combination of Centrifugal assisted AFM and Electrical discharge machining process. The process used EDM principle for producing spark between the rotating electrode and the workpiece surface. In EDM process, spark was generated when two current carrying poles were short circuited. During EDM machining process, metal was eroded from both the poles and formed crater on the workpiece surface. It involved controlled erosion through electrically conductive materials by the starting of rapid and repetitive discharge between both the poles having a gap of less than 0.25 mm between them. In TACAFM process rotating electrode was taken as negative and workpiece was taken as positive terminal. Both the poles were separated by a small gap with a non conductive environment between them, which was developed by the flow of non conductive media (mixture of media and kerosene based oil).

As the pulsed power supply was given to both the poles (rotating electrode and workpiece), free electrons on the rotating electrode were subjected to the electrostatic force. As the free electrons moved towards the work surface, they collide with the media molecules, which break it into positive and negative ion and characterized as plasma. Thus all the positive and negative ions moved towards their opposite polarity. This type of movement of ions could be seen as spark. Figure 1 shows the principle of TACAFM process and ions formation in the plasma channel. If during rotation, electrode make contact with the surface a large intensity current was induced and melted material from the both the poles. As the spark was generated inside the hollow cavity due to potential difference between the rotating electrode and workpiece, high temperature was developed and melted/softened the surface material which could be easily carried out by the abrasive particles.

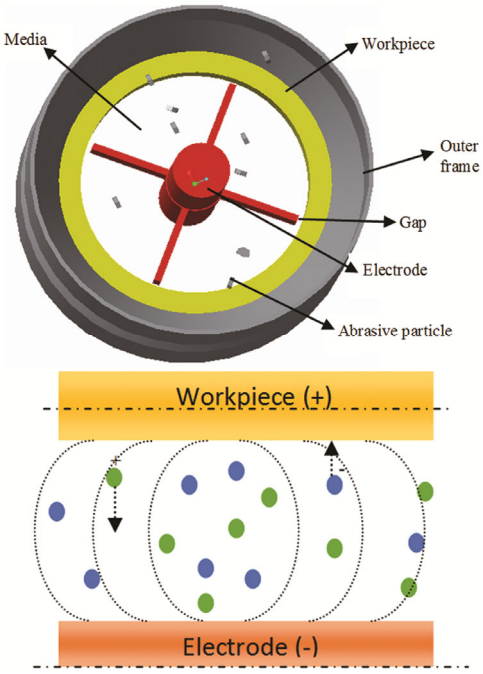

Fig. 1 — Mechanism of material removal in the developed TACAFM process.

2.2 Experimental Setup

The arrangement of the TACAFM process is as shown in Fig. 2. The experimental setup included fixture, 3 phase induction motor, power drive, bearings, gears, manual analog controller (25 Ampere), EDM power supply. The experimental setup of TACAFM process and fixture arrangement is shown in Fig. 2 (a and b) respectively. The fixture was made of nylon and its function was to hold the workpiece and guiding the media between the two opposite media cylinders. The fixture was divided into three parts as shown in Fig. 2(c) and included electrode, bearings and power supply terminals. The rotating electrode was attached through gear which was further rotated by the 3-phase induction motor using intermediate gears as shown in Fig. 2(d). The driving gear was made of mild steel and was fitted to the shaft connected with the 3 phase induction motor. The driving gear was connected with two intermediate gears made of metalon and aluminium and further rotates the gear connected with the electrode.

Basic purpose for making one of the intermediate gears non conductive was to prevent the reverse of the current to the motor. Power drive was used to control the rotation speed of the 3 phase induction motor by changing its frequency of rotation. The function of EDM power supply was to convert the main AC supply to the pulsed DC supply required for the

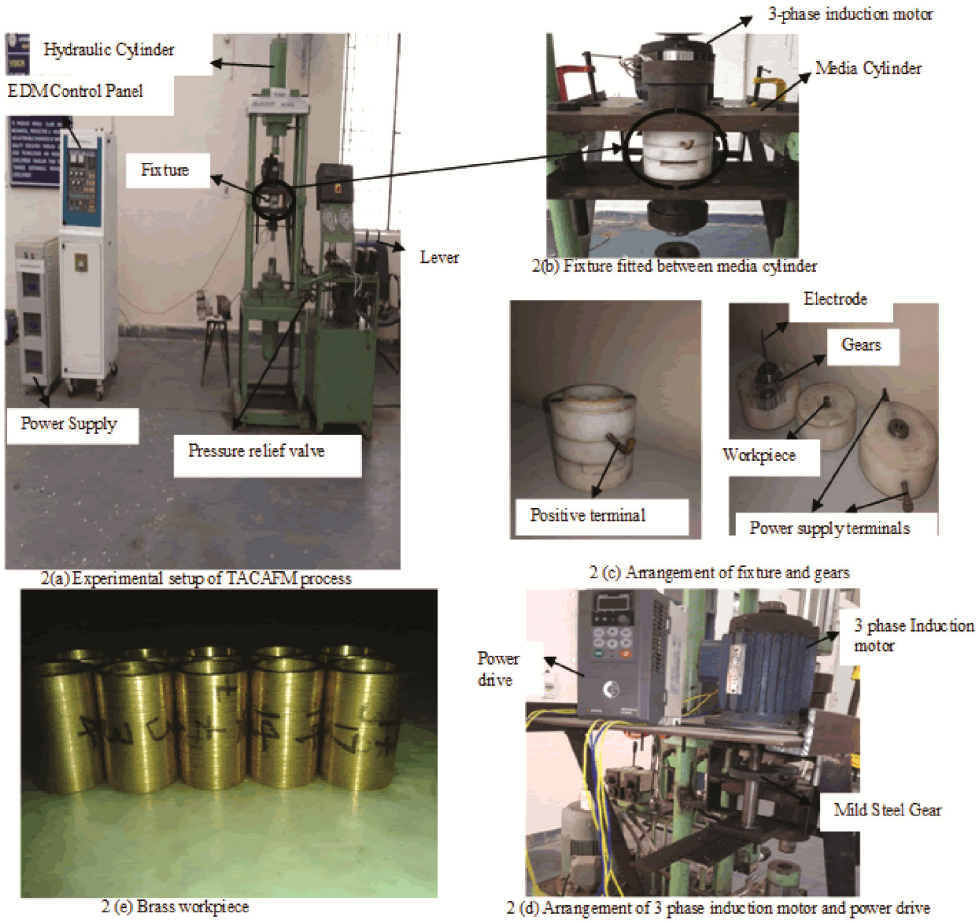

Fig. 2 — Experimental set up of developed TACAFM process.

generation of spark. It also sensed the potential difference between the rotating electrode and the workpiece and helped manual analog controller to sense the gap between both the poles. Whenever the gap was maintained between both the poles spark was generated inside the hollow cavity.

The specification of the pulse generator is as given in Table 1.

2.3 Workpiece

In the present invention brass was used as the workpiece materialbecause it has better malleability and consist low melting point with better flow characteristics. Also it is widely used alloy in the industry such as gears, bearings, valves, marine construction; die making etc. It has a good corrosion resistant property. The brass workpiece and its geometry are as shown in Fig. 2(e) and Fig. 3 respectively.

2.4 Media

The media used for the experimentation is a Non Newtonian media and consist polymer, gel, abrasive particles and kerosene based oil in it. It is visco-elastic in nature and retains its viscosity for a longer duration on the increase of temperature. This increases the abrasive holding capacity of the media and more number of abrasive particles participates in abrasion process. The media also has very less conductivity which permits the lesser spark energy to interact with the workpiece surface to prevent the deterioration in the surface integrity. The properties of the media are as follows:

Viscosity = 0.32 MPa-s, Thermal conductivity = 0.22 W/meter-K, Density = 1219 kg/m^3

Table 1— Specification of pulse generator

Current	25 Ampere
Power Supply	415V, 3 Ph, 50 Hz
Control System	Microprocessor based
Power	3 KVA
MRR Gr-St	180 mm^3/min
MRR Cu-St	140 mm^3/min
Best Surface finish	0.5 µ Ra
Min Electrode Wear	0.3 %
Pulse on Time	1-2000 / 10 steps micro sec
Max Electrode Wt.	50 Kgs

Based on literature survey and pilot experimentations major process parameters as per CCD response surface methodology were selected and trial experiments were performed for analyzing the effect of variable parameters over the responses, i.e. scatter of surface roughness (SSR), micro-hardness and % improvement in R_a. The variable parameters with different levels were presented in Table 2.

The current, duty cycle, rotational speed, extrusion pressure and abrasive concentration were taken as input process variables. The process performance was measured as scatter of surface roughness, micro hardness and % improvement in R_a. A set of 32 experiments according to the CCD of Response surface methodology technique was performed and measured responses were recorded in Table 3. Surface

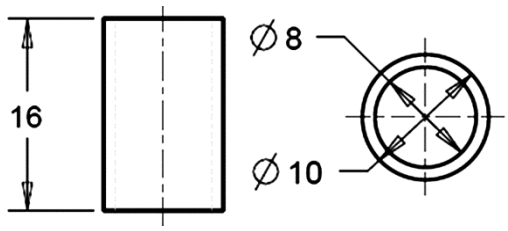

Fig. 3 — Drawing of workpiece geometry.

Table 2 — Control parameters with their limits

Factors	Levels				
	-2	-1	0	+1	+2
A – Current (Ampere)	0	4	8	12	16
B – Duty Cycle (Fraction)	0.63	0.68	0.73	0.78	0.83
C – Rotation (rpm)	100	150	200	250	300
D – Pressure (MPa)	5	10	15	20	25
E – Abrasive Concentration (Fraction)	0.2	0.3	0.4	0.5	0.6

Constant Parameters: Polymer to Gel ratio :1:1, Abrasive particles- Al_2O_3, Mesh Size:180,Temperature - 32± 2 °C, Workpiece Material- Brass, Media Flow Volume – 290 Cm^3

Table 3— Central composite design for the measured experimental results and actual factors

Std	Run	A (Amp)	B (Fraction)	C (rpm)	D (MPa)	E (Fraction)	Initial R_a (µm)	Final R_a (µm)	% Improved R_a	Scatter of Surface roughness (µm)	Micro hardness (HV)
1	3	4	0.68	150	10	0.5	1.21	0.82	31.85	0.82	198.36
2	13	12	0.68	150	10	0.3	1.46	1.06	27.34	0.45	312.86
3	4	4	0.78	150	10	0.3	1.56	1.19	23.22	0.38	221.12
4	12	12	0.78	150	10	0.5	1.33	0.85	36.02	0.42	355.48
5	2	4	0.68	250	10	0.3	1.38	0.95	30.92	0.32	252.12
6	32	12	0.68	250	10	0.5	1.22	0.75	38.45	0.64	332.58
7	15	4	0.78	250	10	0.5	1.16	0.67	41.84	0.43	245.74
8	22	12	0.78	250	10	0.3	1.19	0.69	42.35	0.42	322.14
9	10	4	0.68	150	20	0.3	1.62	1.16	28.67	0.85	212.12
10	5	12	0.68	150	20	0.5	1.41	0.85	40.06	0.39	328.45
11	6	4	0.78	150	20	0.5	1.12	0.79	29.25	0.47	212.97
12	1	12	0.78	150	20	0.3	1.26	0.81	35.66	0.18	301.49
13	27	4	0.68	250	20	0.5	1.20	1.04	13.33	0.32	239.24
14	24	12	0.68	250	20	0.3	1.38	0.94	32.24	0.77	316.47
15	18	4	0.78	250	20	0.3	1.64	1.08	34.24	0.46	256.35
16	17	12	0.78	250	20	0.5	1.57	0.98	37.76	0.44	331.86
17	7	0	0.73	200	15	0.4	1.33	1.15	13.39	0.54	224.48
18	29	16	0.73	200	15	0.4	1.52	1.06	30.37	0.44	412.57
19	11	8	0.63	200	15	0.4	1.46	0.98	33.14	0.45	264.78
20	25	8	0.83	200	15	0.4	1.44	0.83	42.24	0.15	255.47
21	20	8	0.73	100	15	0.4	1.38	0.99	28.53	0.48	272.35
22	23	8	0.73	300	15	0.4	1.28	0.88	30.94	0.54	291.14
23	8	8	0.73	200	5	0.4	1.14	0.70	38.25	0.28	243.87
24	21	8	0.73	200	25	0.4	1.22	0.79	35.24	0.31	245.54
25	14	8	0.73	200	15	0.2	1.56	1.14	27.02	0.78	271.34
26	30	8	0.73	200	15	0.6	1.52	1.08	28.78	0.86	276.67
27	31	8	0.73	200	15	0.4	1.65	1.20648	26.88	0.46	302.34
28	19	8	0.73	200	15	0.4	1.58	1.09573	30.65	0.51	274.82
29	16	8	0.73	200	15	0.4	1.44	1.065024	26.04	0.48	283.57
30	26	8	0.73	200	15	0.4	1.32	1.016664	22.98	0.45	257.37
31	28	8	0.73	200	15	0.4	1.18	0.890428	24.54	0.49	285.56
32	9	8	0.73	200	15	0.4	1.24	0.94426	23.85	0.54	242.23

roughness was measured by Taylor Hobson precision machine (TAYLOR HOBSON SURTRONIC 3+) having resolution of 0.01 micrometer. Surface roughness was measured at five different positions of the work piece and average of these values was taken for the initial and final value of surface roughness. The difference between the maximum R_a value and minimum R_a value was taken as SSR. Micro hardness of the surface was measured by FISCHERSCOPE micro-hardness tester (HM 2000S).

The percentage composition of brass workpiece was shown in Table 4.

2.5 Determination of Number of Abrasive Particles Interacting with the Workpiece Surface

If N_a = Active number of abrasive particles interacting with the workpiece surface

N = Total number of abrasive particles in full volume of media

Then, Total number of abrasive particle in full volume of media $(N)^{21} = \frac{V_a}{V_o}$

where, V_a^{21}= Volume of abrasive particle in full volume of the abrasive laden media = $\frac{C.V_m.d_m}{d_a}$

where, C= concentration of abrasive particle in the media

d_m = density of abrasive laden media

V_m = Volume of abrasive laden media

d_a = Density of abrasive particle

V_o = Unit abrasive particle volume = $\frac{4}{3}.\pi.(\frac{d}{2})^3$

where, d = diameter of abrasive particle

Total number of active abrasive particle interacting with the workpiece surface $(N_a)^{21} = \frac{4.V_a(D.d-d^2)}{V_o.D^2}$,

where, D = Diameter of workpiece

Fraction of abrasive particle involved in cutting action = $\frac{N_a}{N}$

2.6 Determination of Velocity of Impact for Abrasive Particle

In TACAFM process two types of forces are responsible for material removal, i.e axial force (F_a) (direction of media flow) and radial force (F_c) (perpendicular to the workpiece surface). Consider an abrasive particle having mass m entering the passage of the workpiece.

Table 4 — Percentage proportion of basic elements in brass workpiece

Basic Elements	Zn	Cu	Pb	Sn	Ni	Fe
Proportion	36.4	59.2	3.26	1.2	0.4	0.6

If v_a = velocity of abrasive particle by which it is moving in axial direction

and v_c= velocity of abrasive particle by which it is moving towards the inner surface of the workpiece

Centrifugal force developed on abrasive particle due to rotation of electrode F_c^7= m.r.ω^2 = 3π.μ.d.v_c

So $v_c = \frac{F_c}{3\pi.\mu.d}$

If media is passing through the restrictive passage with pressure P, then force applied (F) will be = P . A

where, A = Area of the restrictive passage = $\frac{\pi}{4}.D^2$

If abrasive particle takes time t for passing the restrictive passage then (F) = $\frac{m.v_a}{t}$

Therefore $v_a = \frac{F.t}{m}$

Therefore the resultant velocity of abrasive particle by which it is impacting over the workpiece surface will be the resultant of axial and radial velocity.

$v_R = \sqrt{(v_a)^2 + (v_c)^2}$

3 Results and Discussion

Analysis of Variance technique was used to identify the responses of the selected model. All the significant parameters were identified and the interaction effect of the parameters on the measured responses was studied by the response surface graphs. The regression equation for scatter of surface roughness, micro-hardness and % improvement in R_a was presented in Table 5.

Figure 4 shows a magnificent acceptability of the regression model. Each observed value was comparable to the predicted value obtained from the model. The results of the ANOVA analysis were presented in Tables (6, 7 and 8) respectively. The model F-value of 57.59, 41.79 and 21.63 for scatter of surface roughness, micro hardness and % improvement in R_a respectively, with its Probability > F value less than 0.0001 shows model as significant. There was a 0.01% chance for having a large F-value due to noise. Value of P less than the 0.0500 represented model terms as significant.

For scatter of roughness the terms A, B, AC, AD, BC, BE, CD, CE, DE, B^2, D^2, E^2 were significant model terms with their percentage contribution as 1.32, 17.5, 22.63, 0.61, 3.95, 1.98, 0.88, 0.98, 13, 7.18, 7.56, 22.36 respectively. The values more than 0.1000, showed model terms as insignificant. If more number of insignificant model terms existed, then the model could be improved by the reduction process. The lack of fit values for SSR, micro hardness and %

Table 5 — Regression relation for scatter of surface roughness, micro- hardness and % Improved R_a.

Responses	R^2	Adjusted R^2	Regression Model
Scatter of surface roughness	0.9818	0.9648	SSR = -3.04445 - 0.105313 * A + 19.3259 * B - 0.0179033 * C + 0.116923 * D -7.92013 * E + 0.00056875 * A * C - 0.0009375 * A * D + 0.019 * B * C + 6.75 * B * E + 9e-05 * C * D - 0.00475 * C * E - 0.1725 * D * E - 18.8077 * B^2 - 0.00193077 * D^2 + 8.29808 * E^2
Micro-hardness	0.9447	0.9221	Micro-hardness = 98.8049 + 0.71692 * A + 30.275 * B + 0.519633 * C + 8.1976 * D - 150.733 * E - 0.0450344 * A * C + 22.0016 * A * E + 0.709939 * A^2 - 0.283839 * D^2
% Improved R_a	0.9469	0.9031	% Improved R_a = 745.313 + 0.753073 * A - 1951.96 * B - 0.619535 * C + 0.079125 * D + 147.115 * E + 0.0731562 * A * D + 1.11325 * B * C - 0.0126775 * C * D - 0.377125 * C * E - 4.28125 * D * E - 0.0570378 * A^2 + 1215.96 * B^2 + 0.000420458 * C^2 + 0.112146 * D^2

Current (A), Ampere; Duty Cycle (B), Fraction; Rotational speed of electrode (C), rpm; Extrusion Pressure (D), MPa; Abrasive Concentration (E), Fraction

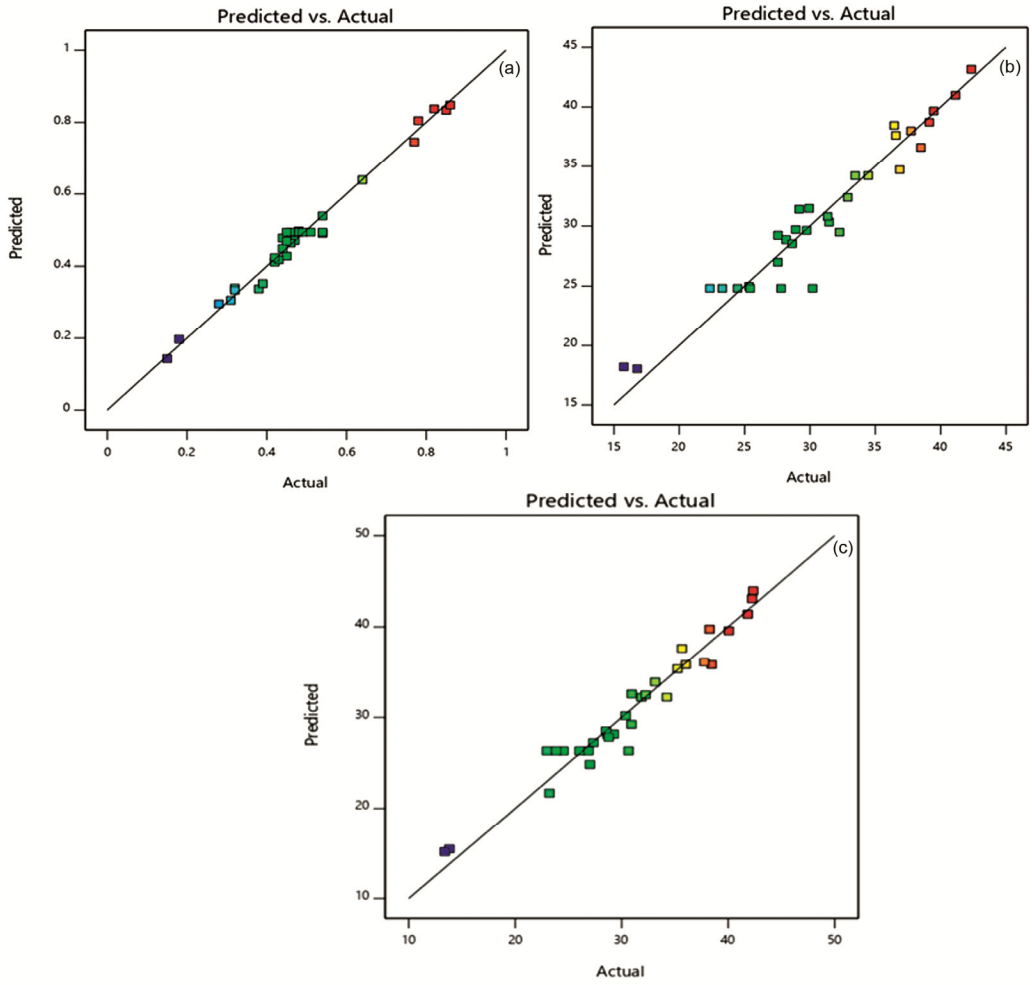

Fig.4 — (a) Predicted and actual responses for scatter of surface roughness, (b) Predicted and actual responses for micro-hardness, and (c) Predicted and actual responses for % Improved R_a.

improvement in R_a were found as 0.99, 0.18, and 0.52, respectively, showing the developed model for SSR, micro-hardness and % improvement in R_a as adequate and satisfactory.

The adequacy of the model fit can be observed by the value of R^2. The determination coefficient for scatter of surface roughness is observed as 0.9818, showing the developed model is significant for predicting the

Table 6 — ANOVA outcome for fitted RSM model for Scatter of surface roughness

Source	Sum of Squares	Degree of Freedom	Mean Square	F- value	Probability>F	
Model	0.9437	15	0.0629	57.59	< 0.0001	Significant
A	0.0121	1	0.0121	11.12	0.0042	
B	0.1601	1	0.1601	146.52	< 0.0001	
C	0.0001	1	0.0001	0.0610	0.8080	
D	0.0001	1	0.0001	0.1373	0.7158	
E	0.0028	1	0.0028	2.58	0.1279	
AC	0.2070	1	0.2070	189.51	< 0.0001	
AD	0.0056	1	0.0056	5.15	0.0374	
BC	0.0361	1	0.0361	33.05	< 0.0001	
BE	0.0182	1	0.0182	16.68	0.0009	
CD	0.0081	1	0.0081	7.41	0.0150	
CE	0.0090	1	0.0090	8.26	0.0110	
DE	0.1190	1	0.1190	108.95	< 0.0001	
B^2	0.0657	1	0.0657	60.13	< 0.0001	
D^2	0.0692	1	0.0692	63.37	< 0.0001	
E^2	0.2046	1	0.2046	187.30	< 0.0001	
Residual	0.0175	16	0.0011			
Lack of Fit	0.0120	11	0.0011	0.9944	0.5414	Not Significant
Pure Error	0.0055	5	0.0011			
Cor Total	0.9612	31				
Std. Dev.	0.0331		R^2	0.9818		
Mean	0.4850		Adjusted R^2	0.9648		
C.V. %	6.81		Predicted R^2	0.9006		
Press	0.0955		Adequate Precision	30.1653		

Table 7 — ANOVA outcome for fitted RSM model for micro-hardness

Source	Sum of Squares	Degree of Freedom	Mean Square	F- value	Probability>F	
Model	64135.16	9	7126.13	41.79	< 0.0001	Significant
A	54101.56	1	54101.56	317.28	< 0.0001	
B	54.99	1	54.99	0.3225	0.5759	
C	1523.70	1	1523.70	8.94	0.0068	
D	60.52	1	60.52	0.3549	0.5574	
E	153.37	1	153.37	0.8994	0.3532	
AC	1297.98	1	1297.98	7.61	0.0115	
AE	1239.22	1	1239.22	7.27	0.0132	
A^2	3853.61	1	3853.61	22.60	< 0.0001	
D^2	1503.88	1	1503.88	8.82	0.0071	
Residual	3751.41	22	170.52			
Lack of Fit	1437.07	17	84.53	0.1826	0.9965	Not significant
Pure Error	2314.34	5	462.87			
Cor Total	67886.57	31				
Std. Dev.	13.06		R^2	0.9447		
Mean	276.36		Adjusted R^2	0.9221		
C.V. %	4.73		Predicted R^2	0.9143		
Press	5817.13		Adequate Precision	28.3475		

variation on scatter of surface roughness up to 98.18 percent, and the model is able to demonstrate the process. However the Predicted R^2 of 0.9006 has a good relation with the adjusted R^2 of 0.9648. The lower value (6.81) of CV % shows better accuracy and consistency of the performed experiments. Adequate precision for the model as 30.16, was more than 4, which shows an adequate signal.

For micro hardness terms A, C, AC, AE, A^2, D^2 were significant model terms with their percentage

Table 8 — ANOVA outcome for fitted RSM model for % Improved R_a

Source	Sum of Squares	Degree of Freedom	Mean Square	F- value	Probability>F	
Model	1518.41	14	108.46	21.63	< 0.0001	Significant
A	337.73	1	337.73	67.37	< 0.0001	
B	126.91	1	126.91	25.32	0.0001	
C	24.75	1	24.75	4.94	0.0402	
D	28.84	1	28.84	5.75	0.0282	
E	13.40	1	13.40	2.67	0.1205	
AD	34.25	1	34.25	6.83	0.0182	
BC	123.93	1	123.93	24.72	0.0001	
CD	160.72	1	160.72	32.06	< 0.0001	
CE	56.89	1	56.89	11.35	0.0036	
DE	73.32	1	73.32	14.62	0.0014	
A^2	24.60	1	24.60	4.91	0.0407	
B^2	272.96	1	272.96	54.45	< 0.0001	
C^2	32.64	1	32.64	6.51	0.0206	
D^2	232.19	1	232.19	46.32	< 0.0001	
Residual	85.22	17	5.01			
Lack of Fit	47.14	12	3.93	0.5157	0.8389	Not significant
Pure Error	38.09	5	7.62			
Cor Total	1603.64	31				
Std. Dev.	2.24		R^2	0.9469		
Mean	30.83		Adjusted R^2	0.9031		
C.V. %	7.26		Predicted R^2	0.8275		
Press	276.67		Adequate Precision	18.7774		

contribution as 85.17, 2.39, 2.04, 1.95, 6.06, and 2.36, respectively. The values more than 0.1000, showed model terms as insignificant. If more number of insignificant model terms existed, then the model could be improved by the reduction process. This case had 99.65 % chance of having large Lack of Fit F-value due to noise. Predicted R^2 of 0.9143 was in a close relation with the Adjusted R^2 of 0.9221; i.e. the difference between them was less than 0.2. The small value (6.81) of CV % shows better accuracy and consistency of the performed experiments. Adequate Precision showed the value of S/N ratio. The ratio more than 4 was advisable. The ratio of 28.347 represented an adequate signal.

For % improvement in R_a terms A, B, C, D, AD, BC, CD, CE, DE, A^2, B^2, C^2, D^2 were significant model terms with their percentage contribution as 21.88, 8.22, 1.6, 1.86, 2.22, 8.03, 10.42, 3.68, 4.75, 1.59, 17.69, 2.12 and 15.05, respectively. The values more than 0.1000, showed model terms as insignificant. If more number of insignificant model terms existed, then the model could be improved by the reduction process. This case had 83.89 % chance of having large Lack of Fit F-value due to noise. Predicted R^2 of 0.8275 was in a close relation with the Adjusted R^2 of 0.9031; i.e. the difference between them was less than 0.2. The small value (7.26) of CV % shows better accuracy and consistency of the performed experiments. Adequate Precision showed the value of S/N ratio. The ratio more than 4 was advisable. The ratio of 18.777 represented an adequate signal.

Figure 4 shows the plot across the actual and predicted responses. It was observed that the results between both the responses were very close for SSR, micro-hardness and % improvement in R_a. It shows the predicted model was acceptable.

The perturbation graph presented in Fig. 5 (a), shows the effect of variable process parameters on the SSR. The midpoint indicated as (value 0), in design expert shows reference point for all the parameters. The keen slope for the parameters current (A), duty cycle (B), rotational speed (C), pressure (D), abrasive concentration (E) shows that these parameters are highly dependent on scatter of surface roughness. The reason for this circumstance was discussed while demonstrating the interaction effects of parameters. Table 6, Table 7 and Table 8 shows the interactions, in which current (A), duty cycle (B), current and rotational speed (AC), current and extrusion pressure (AD), duty cycle and rotational speed (BC), duty cycle and abrasive concentration (BE), rotational

speed and extrusion pressure (CD), rotational speed and abrasive concentration (CE), extrusion pressure and abrasive concentration (DE) were the interactions for scatter of surface roughness while current (A), rotational speed (C), current and rotational speed (AC), and current and abrasive concentration (AE) were the interactions for the micro-hardness and also current (A), duty cycle (B), rotational speed (C), extrusion pressure (D), Current and extrusion pressure (AD), duty cycle and rotation (BC), rotation and extrusion pressure (CD), rotation and abrasive concentration (CE), extrusion pressure and abrasive concentration (DE) were the interactions for the % improvement in R_a. The relevant plots to these interactions were shown from Fig. 5 (b-h) for scatter of surface roughness, from Fig. 6 (b and c) for micro-hardness and from Fig. 7(b-f) for % improvement in R_a,respectively.

Figure 5 (b) shows as the value of current and rotational speed increased, scatter of surface roughness decreased keeping other parameter as constant. Due to increase in the current value, discharge energy density also enhanced which means, for each pulse higher amount of energy could be available for melting the work surface. This developed high temperature on the surface and formed deeper craters on it [22]. When abrasive particles came in contact with the melted material, less amount of force was required for removing the molten/semi molten material from the surface. This provided good

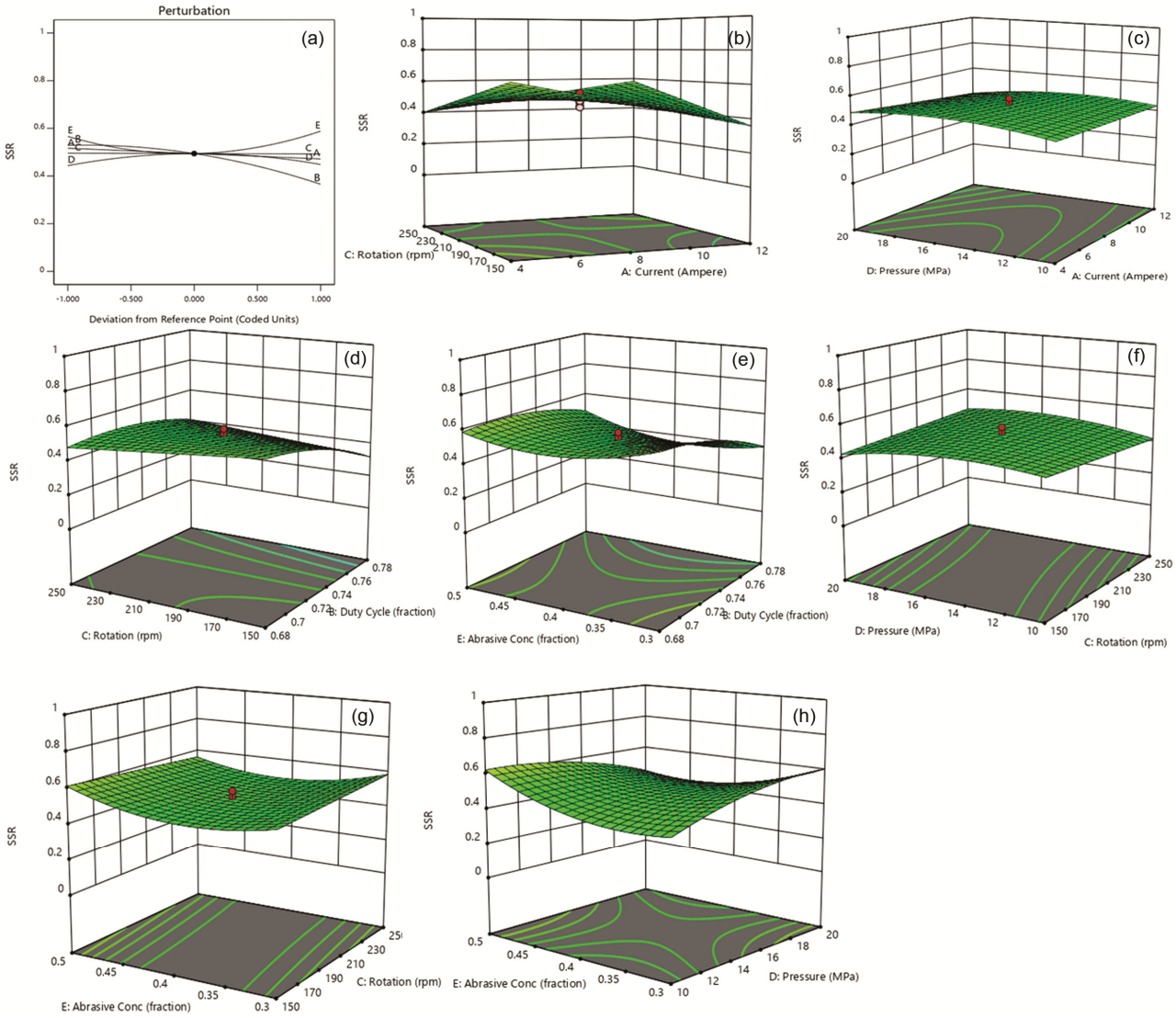

Fig. 5 — (a) Perturbation plots for scatter of surface roughness, (b - h) Response 3D surface plot showing the interactive influence of variable parameters for scatter of surface roughness.

level of finishing and decreased the scatter of roughness. As the rotational speed of electrode was increased, it developed a centrifugal force of larger magnitude in the media flow path. This may cause more number of abrasive particles contacting the workpiece surface. Therefore number of dynamic abrasive particles participating in material removal can increase that leads increase in the resultant force applied by the abrasive particles. Due to increase in the resultant force, abrasive particles can easily remove the molten/semi molten state material from the surface and produced good level of finishing with reduced scatter of roughness of the workpiece surface [23]. Figure 5 (c) shows as the extrusion pressure and current was increased; scatter of roughness increased. As the value of current was increased, a huge temperature was developed on the surface. A large energy pulse of EDM produces deeper crater on the surface and causes larger material removal. Therefore, large value of material removal leads to deteriorate the surface quality and increases the value of scatter of roughness. As Fig. 5(d) shows increase in scatter of surface roughness with extrusion pressure. It can be said that as the extrusion pressure was increased, the abrasive particles impacted the surface with larger force and caused deep cut on the surface. These deeper cut enhanced the material removal; lager material removal led to decrease in surface integrity. This increased the value of scatter of surface roughness. The similar trend was also observed by Walia *et al.* in 2006 [23]. Figure 5(d) shows decrease in scatter of surface roughness with rotation and duty cycle, while keeping other parameters as constant. As duty cycle increased, the spark frequency enhanced due to availability of discharge energy for a longer duration. Larger amount of discharge energy developed high temperature on the workpiece surface and melted more material, which could be easily removed by the abrasive particles in form of micro-chips. This reduced the value of scatter of roughness. Figure 5(e) also shows initially decrease and further increase in scatter of surface roughness value with abrasive concentration. As the abrasive concentration increased, numbers of active abrasive particles participating in the abrasion process were increased. This increased the available energy for breaking the atomic bond of the material and developed new surface by displacing the atoms [24]. This caused increase in MR and provided better surface finish, which reduced the scatter of surface roughness. However on further increasing the abrasive concentration, large number of abrasive particles participates in the abrasion and leads to improvement in material removal which corresponded deterioration in surface finish. This increased the scatter of surface roughness. Figure 5(f) shows that as the extrusion pressure is increased, scatter of roughness initially increased and further decreased. However there is very negligible change in the response with respect to the rotational speed keeping other parameters constant. The reason may be that at lower extrusion pressure both material removal and surface finish are low because shearing energy required by the abrasive particles is not enough to shear the peaks. Shearing strength of the sharp edged abrasive particles should be greater than the strength of material for more material removal. This increased the scatter of surface roughness, while on further increasing the extrusion pressure abrasive particles imparted a larger force on the surface and corresponded more material removal along with better surface integrity. This reduced the value of scatter of surface roughness [23]. Figure 5(g) shows that there was initially decrease and then further increase in scatter of roughness with increasing abrasive concentration. However there was some increase in scatter of roughness with respect to the rotation. The reason may be that on enhancing the abrasive concentration in the media, more abrasive particles interacted with the finishing surface and performed efficient cutting action. This improved the material removal and surface finish which corresponded decrease in scatter of surface roughness. On further increasing the abrasive concentration surface finish deteriorated due to more material removal. This increased the scatter of surface roughness of the surface. Figure 5(h) shows increase in scatter of roughness with the extrusion pressure and abrasive concentration while keeping other parameters as constant.

The perturbation graph presented in Fig. 6(a), shows the effect of variable parameters over the micro-hardness of surface. Figure 6(b) shows effect of current intensity and rotational speed on the micro-hardness of the material keeping other parameter constant. In TACAFM process increase in micro hardness with current occurred due to heating and better quenching. The spark generation in TACAFM process developed large amount of heat in the finishing zone. The huge amount of heat caused better quenching of material and facilitated hard carbides

and other hardened compounds formation over the surface. These hardened compounds developed over the surface increased the micro hardness of the surface which was similar with the results obtained by Gill and Kumar [25].

Figure 6(b) shows as the rotational speed was increased, micro hardness of the surface also increased. In TACAFM process two forces (axial and radial) are acting during the finishing process and resultant of these two forces may be responsible for the material removal mechanism. On increasing the rotational speed, radial component of force increases which enhances the resultant force. Therefore abrasive particles were thrown on the surface with larger force due to the involvement of the centrifugal force during the media flow. It caused work hardening of the surface and increased the micro hardness of finishing surface. The similar results were also obtained by Walia *et al.* in 2008 [26]. Fig. 6(c) shows as the current intensity was increased, micro hardness of the surface also increased. On increasing the current intensity more melting was done on the workpiece surface which caused work hardening of the surface. This work hardening increased the micro hardness of the surface. Fig. 6(c) also shows that micro hardness of the surface was enhanced due to increase in abrasive concentration. On increasing the abrasive concentration, more and more abrasive particles impacted on the workpiece surface which induced a residual stress over the surface and enhanced the micro hardness of surface.

The perturbation graph presented in Fig. 7(a), shows the effect of variable parameters over the % improvement in surface roughness. Figure 7(b) shows as the current intensity and extrusion pressure is increased keeping other parameters constant, surface finish gets better. As the current intensity is increased, discharge energy density is also increased. This causes availability of higher energy for each pulse which corresponds rapid melting of surface due to increase of temperature over the surface. This rapid melting of surface produces deeper craters on it [22], which can be easily carried away by the abrasive particles and provides good level of finish.

In conventional AFM process only axial force is responsible for the material removal which acts in the direction of media flow. But TACAFM process is a combination of Centrifugal force assisted AFM (CFAAFM) and EDM process. In the present developed process axial force and radial force both are responsible for the material removal. Radial force acts in the direction perpendicular to the surface. The resultant force subjected by the abrasive particles will be the resultant of axial and radial forces. Initially at lower pressure the resultant force is less and the abrasive particles are not able to shear the peaks of the surface. But as the pressure is increased, the resultant force also increases and removes more material which improves the surface finish. Figure 7(c) shows increase in surface finish with duty cycle and rotation keeping other parameter constant. As the duty cycle is increased, discharge energy may be applied for a longer duration. It can develop high temperature over the surface and softens more volume of material. This soft material can be easily carried by the abrasive particles with lesser amount of force that causes more material removal and provide good surface finish. As the rotational speed of the electrode is increased radial force increases which causes increase in resultant force. This may cause more availability of energy to break the atomic bond and will develop new surface with better surface integrity which was similarly observed by Walia *et al.* (2006) [24]. Figure 7(d) shows improvement in surface finish

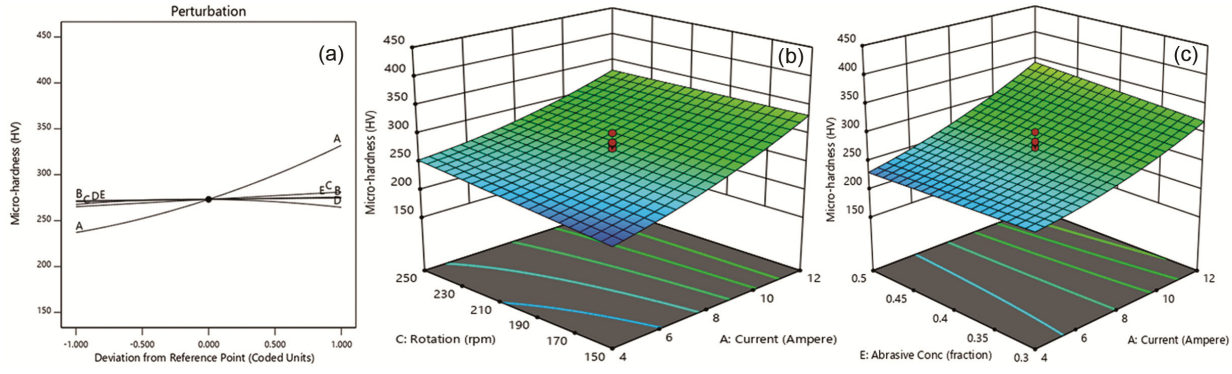

Fig. 6 — (a) Perturbation plots for micro-hardness, (b - c) Response 3D surface plot showing the interactive influence of variable parameters for micro-hardness.

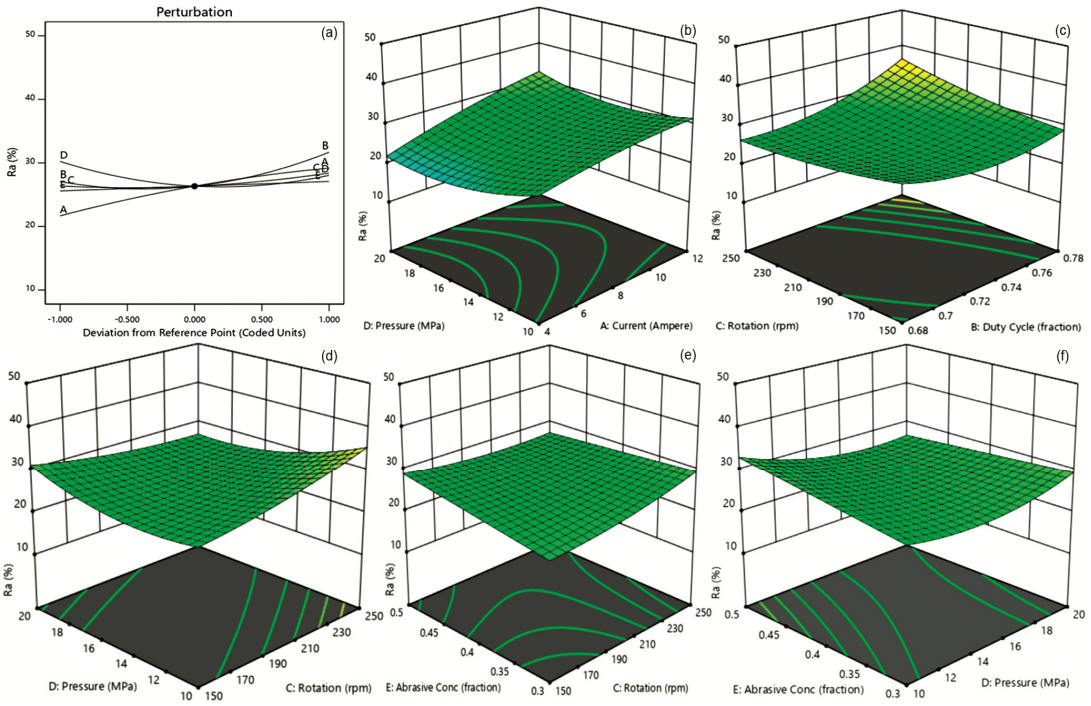

Fig. 7 — (a) Perturbation plots for % improved R_a, (b - f) Response 3D surface plot showing the interactive influence of variable parameters for % Improved R_a.

with rotation and pressure keeping other parameter constant. This is due to the increase in the resultant force by which the abrasive particles are impacting over the surface. Figure 7(e) shows as the rotation and abrasive concentration in increased, percentage improvement in surface finish also increases. On increasing the abrasive concentration, dynamic number of abrasive particles is increased and more number of abrasive particles may come in contact with the surface. This can also increase the contact region between the abrasive particles and workpiece surface. More number of abrasive particles can easily remove the peak of the surface and provide good level of surface finish. The results are comparable to the results obtained by Gorana *et al.* (2004) [27]. However, on further increase of abrasive concentration, dynamic abrasive particles are increased but the interference between the abrasive particles also increases leading to energy loss and reduction in rate of material removal will reduce. Figure 7(f) shows as the pressure and abrasive concentration is increased, percentage improvement in surface finish also increases. This might be due to increase in active abrasive particles.

3.1 Optimization

Optimization was performed to minimize scatter of surface roughness (SSR), maximize micro-hardness and maximize % improvement in R_a having the constrained limit of five factors as shown in Table 2. The optimization was performed by using Design expert software. The desirability factor was in the range of 0 to 1, in which the smallest value shows the low desirable factor. The process variables with ultimate desirability mean it has optimum variable setting. The optimum values for the input parameters and their corresponded responses were analyzed by the software and the details were presented in Table 9. For single factor optimization, other response variables were neglected while in case of multivariable optimization, all the responses were considered and provided the equivalence significance. For the validation of optimized responses confirmation experiments were performed as shown in Table 9. It was seen from the experimental validation predicted values were very close to the experimental values.

3.2 Calculation of Number of Abrasive Particle Interacting with the Workpiece Surface

For the optimized condition,

C = 0.5, V_m = 290e-6 m^3, d_m =1219 kg/m^3, d_a = 1340 kg/m^3, d = 33 microns, D = 8e-3m,

Putting the above values, V_a= 1.32e-4 m^3, V_o = 0.188e-13 m^3

Number of abrasive particle interacting with the workpiece surface, N_a = 1.153e8

Table 9 — Single factor and multifactor optimization and comparative study of optimized outcomes and experimental facts of process variables

Optimization type	Objective	Optimized process variables					Response (predicted)	Response (Experimental)	Desirabilty
		Current (Amp)	Duty cycle (Fraction)	Rotational speed (rpm)	Pressure (MPa)	Abrasive concentration (Fraction)			
Single Response	To minimize SSR	11.832	0.778	150.3	11.024	0.343	0.1497 µm	0.15 µm	0.828
Single Response	To maximize Micro-hardness	12	0.78	150.746	14.506	0.5	345.963 HV	345.951 HV	0.689
Single Response	To maximize % Improved R_a	11.696	0.78	248.621	11.115	0.326	42.44%	39.52%	1.000
Multi response	To minimize SSR, maximize Micro-hardness and maximize % Improved R_a	12	0.78	150	19.944	0.5	0.142µm, 336.038 HV and 38.52%	0.15 µm and 335.175 HV and 35.02%	0.8

Number of abrasive particle in full volume of media, N = 70.21e8

Fraction of abrasive particle involved in material removal = $\frac{N_a}{N}$ = 0.016

3.3 Calculation of Velocity of Impact

m^7= 2.6e-7 kg, r = 16.5e-6m, N = 150 rpm, ω = 15.707 rad/s

So, F_c = 1.0583e-9N

Therefore, v_c = 1.56e-10 m/s

If t = 2e-6 sec, then v_a = 6.7e-5 m/s

So, impact velocity will be = 6.7e-5 m/s

3.4 SEM Analysis

The work pieces finished by TACAFM process were studied by scanning electron microscopy. SEM analysis was done for analyzing the microstructure of the workpiece profile at 500 X magnification. Figure 8 shows the microstructure images of the workpiece during and after the finishing in TACAFM process. Figure 8(a) shows the SEM image of surface before finishing. In TACAFM process material removal occurs due to thermal evaporation, melting and abrasion mechanism. When the spark is generated between the rotating electrode and finishing surface, oxide formation occurred due to presence of atmospheric gases in the finishing zone. The surface imperfections such as oxide layers, recast layers could be seen on the surface as revealed in Fig. 8(b). The formation of oxide layers on the surface leads to poor electrical conductivity of the workpiece and further hampers the machining process. The continuous flow of media in the gap, made nearly about an oxygen free environment around the finishing zone. The abrasive laden media had a high dielectric resistance which corresponded negligible breakdown during the machining and further ionize on the collision of electrons with the molecules. The spark developed high temperature in the finishing zone and melted the material on the surface. Figure 8(b) shows the craters developed on the surface due to EDM mechanism. When the electrode is kept stationary, it develops spark at a particular position where surface is nearer to the electrode tip and deteriorate the surface quality. Therefore rotation of electrode is necessary to maintain the uniformity over the surface. Figure 8(b) clearly shows the molten/ semi molten material and spark craters on the surface during the electrode rotation. These soften material required less amount of force by abrasive particles to take away from the surface. Figure 8(c) shows surface structure was improved after the finishing and no cracks were observed on the surface, although some abrasive particles cutting marks were observed on the surface infrequently.

3.5 XRD Results

X-ray diffraction technique was used for the micro structural study of the finished surface. X-ray diffraction technique analysis of finished workpiece was performed with a software tool "X'Pert High Score". XRD graph of finished brass workpiece was shown in Fig. 9. It can be observed from the XRD graphs that maximum peaks were identified for copper magnesium oxide and copper oxide at 2θ of 42.32 degree on (200) plane and had a cubic crystal system. Also some more peaks were identified for Copper oxide at 2θ of 36.44 degree and 52.48 degree

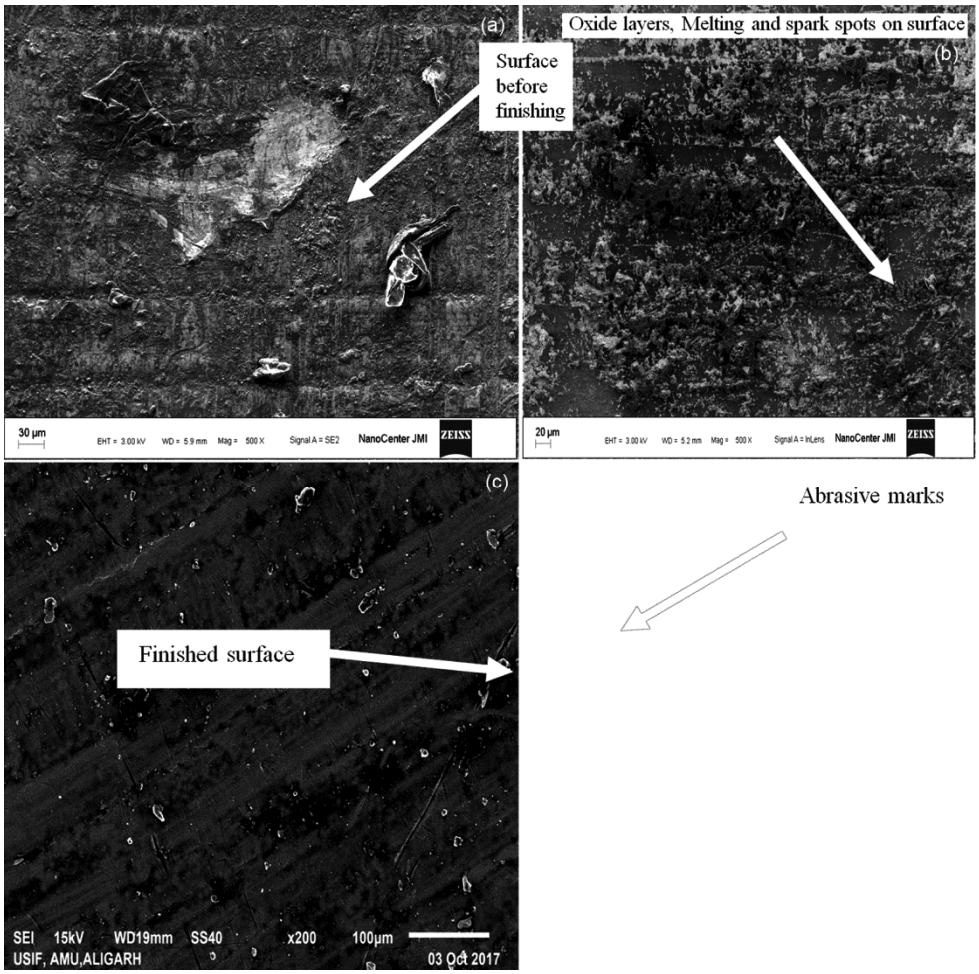

Fig. 8 — (a) SEM image of surface before finishing, (b) Oxide layers formation and Spark spots during the electrode rotation, and (c) SEM image of finished surface.

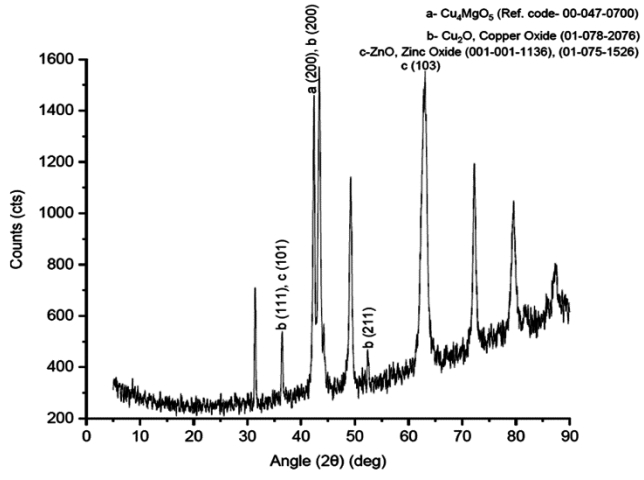

Fig. 9 — XRD results of surface produced by TACAFM process.

at plane (111), (211) respectively with a cubic crystal system. Zinc Oxide peaks were identified at 2θ of 36.49 degree and 63.102 degree at plane (101), (103) respectively. Both were having hexagonal crystal system. During the XRD interpretation some groups with lower peaks were discounted.

4 Conclusion

In the present work, brass workpiece was finished using the developed Thermal additive Centrifugal AFM process. Experiments were performed for the input parameters such as current, duty cycle, rotational speed, extrusion pressure and abrasive concentration against responses scatter of surface roughness, micro-hardness of surface and % improvement in R_a. The results were obtained from the regression correlations and software tools. The conclusions drawn on the basis of the above study are:

- Duty cycle and current intensity have the major effect on finishing performance in comparison of the other input parameters.
- Duty cycle has the highest contribution of 17.5 % on the scatter of surface roughness. Scatter of

roughness decreased on increasing the duty cycle. The best scatter of roughness value obtained for the brass workpiece was 0.15 μm.

- Current has the largest contribution of 85.17 % against the micro-hardness of surface. On increasing the current, micro-hardness of the surface was increased. The best micro-hardness of the surface was achieved as 332.58 HV.
- Current has the largest contribution of 21.88% against % improvement in R_a. On increasing the current intensity, more material removal was obtained due to more number of craters formed by the EDM mechanism on the surface. This makes easier for the abrasive particles to take away the material and provide good level of finish. The best % improvement in R_a was 39.52%.
- A fraction of 0.016 abrasive particles have participated in material removal.
- The process is capable of removing the craters and cracks on the surface at higher values of variables.

References

1 Tan K L, Yeo S H,& Ong C H, *Proc Inst Mech Eng B J Eng Manuf,* 271 (2016) 2302.

2 Singh G, Singh A K, & Garg P, *Mater Manuf Process,*32 (2016) 581.

3 Singh S, *Studies in metal finishing with magnetically assisted abrasive flow machining, Ph. D thesis, IIT Roorkee,* 2002.

4 Subramanian KT ,& Balashanmugam N, *Int J Adv Manuf Technol,* 85 (2016) 2189.

5 Han S, Salvatore F, & Rech J, *J Mater Process Technol*, 267 (2018) 348.

6 Tzeng Hsinn Jyh, Yan Biing-Hwa, Hsu Rong-Tzong, & Lin Yan-Cherng, *Int J Adv Manuf Technol,* 34 (2007) 649.

7 Mittal S, Kumar V, & Kumar H, *Mater Manuf Process,* 30 (2015) 902.

8 Wan S, Ang Y J, Sato T, & Lim G C, *Int J Adv Manuf Technol,* 71 (2014) 1077.

9 Chen K Y, & Cheng K C, *Int J Adv Manuf Technol,* 74 (2014) 781.

10 Fu Y, Wang X, Gao H, Wei H, & Shichong L, *Int J Adv Manuf Technol,* 84 (2016) 1725.

11 Mali H S, & Manna A, *Int J Adv Manuf Technol,* 50 (2010) 1013.

12 Lv Z, Hou R, Huang C, Zhu H, & Qi H, *Int J Adv Manuf Technol*, 100 (2019) 2021.

13 Wang X C, Wang C C, Wang C Y, & Sun F H, *Chin. J Mech Eng*, 31 (2018) 97.

14 Shao Y, & Cheng K, *Int J Adv Manuf Technol*, 105 (2019) 4571.

15 Sankar M R, Jain V K, & J Ramkumar, *Int J Mach Tools Manuf*, 50 (2010) 637.

16 Sankar M R, Mondal S, Ramkumar J, & Jain V K, *Int J Adv ManufTechnol,* 42 (2009) 678.

17 Brar B S, Walia R S, Singh V P, & Sharma M, *J Inst Eng India Ser C*94 (2013) 21.

18 Walia R S, Shan H S, & Kumar P K*, Int J Adv Manuf Technol,* 44 (2009) 700.

19 Marzban M Ali, & Hemmati Seyed Jalal, *Int J Adv Manuf Technol,* 89 (2017) 125.

20 Tzeng Hsinn Jyh, Yan Biing Hwa, Hsu Rong Tzong, & Lin Yan Cherng, *Int J Adv Manuf Technol*, 32 (2007) 1163.

21 Walia R S, Shan H S, & Kumar P K, *Int J Ad Manuf Technol,* 38 (2008) 1157.

22 Yan B H, Tsai H C , & Huang F Y, *Int J Mach Tools Manuf,* 45 (2005) 194.

23 Walia R S, Shan H S, & Kumar P, *Mater Manuf Process,* 21 (2006) 375.

24 Walia R S, Shan H S, & Kumar P, *Mach Sci Technol,* 10 (2006) 1.

25 Gill A S, & Kumar S, *Mater Manuf Process,* 31 (2016) 514.

26 Walia R S, Shan H S, & Kumar P, *Int J Adv Manuf Technol,* 39 (2008) 1171.

27 Gorana V K, Jain V K, & Lal G K, *Int J Mach Tools Manuf*, 44 (2004) 201.